

DEVELOPMENT AND DISEASE

Ectopic expression of *Gcm1* induces congenital spinal cord abnormalities

Brahim Nait-Oumesmar¹, Barbara Stecca¹, Girish Fatterpekar², Thomas Naidich², Joshua Corbin^{1,*} and Robert A. Lazzarini^{1,†}

¹Department of Molecular, Cellular and Developmental Biology and ²Department of Radiology, Mount Sinai School of Medicine, One Gustave L. Levy Place, New York, NY 10029, USA

*Present address: Skirball Institute, New York University, New York, NY, USA

†Author for correspondence (e-mail: robert.lazzarini@mssm.edu)

Accepted 9 April 2002

SUMMARY

Brief ectopic expression of *Gcm1* in mouse embryonic tail bud profoundly affects the development of the nervous system. All mice from 5 independently derived transgenic lines exhibited either one or both of two types of congenital spinal cord pathologies: failure of the neural tube to close (spina bifida) and multiple neural tubes (diastematomyelia). Because the transgene is expressed only in a restricted caudal region and only for a brief interval (E8.5 to E13.5), there was no evidence of embryonic lethality. The dysraphisms develop during the period and within the zone of transgene expression. We present evidence that these dysraphisms result from an

inhibition of neuropore closure and a stimulation of secondary neurulation. After transgene expression ceases, the spinal dysraphisms are progressively resolved and the neonatal animals, while showing signs of scarring and tissue resorption, have a closed vertebral column. The multiple spinal cords remain but are enclosed in a single spinal column as in the human diastematomyelia. The animals live a normal life time, are fertile and do not exhibit any obvious weakness or motor disabilities.

Key words: *glial cells missing*, Secondary neurulation, Cell fate specification, Neural tube defects, Tail bud, Mouse

INTRODUCTION

The neuroectodermal cells of the primitive neural tube are the common progenitor cells of the neurons and glia of the CNS. In *Drosophila*, the transcription factor Glial cells missing (*Gcm*) is believed to play a central role in the cell-fate specification of neurons and glia (Hosoya et al., 1995; Jones et al., 1995). The observations that *Drosophila* embryos with an impaired *gcm* gene are impoverished of glia, while embryos ectopically expressing *gcm* have an excess of glia, usually at the expense of neurons, have led to the proposition that *gcm* is a binary switch controlling the flow of progenitor cells into glial or neuronal cell lineages. We and other have identified two vertebrate homologues of *gcm*, named *Gcm1* and *Gcm2* (also called *Gcma* and *Gcmb*, respectively) (Akiyama et al., 1996; Altshuller et al., 1996; Basyuk et al., 1999; Kim et al., 1998). Mammalian *Gcm1* and *Gcm2* share a highly conserved DNA binding domain with the *Drosophila gcm* which does not resemble known DNA binding domains. Consistent with their nuclear localization and specific DNA-binding to the motif 5'-AT(G/A)CGGGT-3', *Gcm* proteins were proposed to be a novel class of transcription factors (Schreiber et al., 1997; Schreiber et al., 1998). Surprisingly, the mammalian *Gcm1* and 2 are more highly expressed in non-neuronal tissue than in brain. However, both *Gcm1* and 2 are expressed in the mammalian developing CNS. Furthermore, the mouse *Gcm1* can fulfill

many of the functions of the *Drosophila gcm* gene when introduced into the fly (Kim et al., 1998; Reifegerste et al., 1999). Thus, ectopic expression of mouse *Gcm1* in *Drosophila gcm* null mutant embryos induces gliogenesis. A direct assessment of the role of the mouse *Gcm1* gene is complicated by the fact that *Gcm1* null mutant conceptuses fail to develop a competent placenta (Anson-Cartwright et al., 2000; Schreiber et al., 2000) and die at E10, a time well before gliogenesis occurs.

We have assessed the potential role of *Gcm1* in murine CNS development using transgenic mice that express *Gcm1* under the control of the mouse *Hoxa7* enhancer. We show that ectopic expression of *Gcm1* during early embryogenesis leads to two severe neural tube defects that have counterparts in human disease: failure of the neural tube to close (spina bifida or more precisely, myelocoele) and multiple neural tubes (diastematomyelia). The dysraphisms develop during the period of transgene expression and within the zone of expression. After transgene expression ceases, the dysraphisms are progressively resolved and the open neural tube closes. Neonatal animals, while showing signs of scarring and tissue resorption, have a closed vertebral column containing the multiple neural tubes (as in human diastematomyelia). The animals live a normal life span, are fertile and do not exhibit any obvious weakness or motor disabilities.

MATERIALS AND METHODS

Hoxa7-Gcm1 transgene construct

An *AccI-EcoRI* cDNA fragment containing the entire coding sequence of *Gcm1* was blunt-ended and cloned into *SmaI* site of Bluescript SKII, generating p*Gcm1*. A 190-bp *SpeI* fragment containing the SV40 polyadenylation signal was directionally cloned at the 3' end of the *Gcm1* coding region creating the p*Gcm1*/SV40 plasmid. The *Hoxa7-Gcm1* transgene was created by inserting the *Hoxa7* enhancer and the TK minimal promoter from the pAX470 plasmid (gift from P. Gruss) (Fig. 1A).

Generation of transgenic mice

The entire transgene was released from the *Hoxa7-Gcm1* plasmid by digestion with *ClaI* and *SacII*. A transgene containing *lacZ* instead of *Gcm1* was obtained from pAX470 plasmid by digestion with *HindIII* and *SnaBI*. These fragments were gel purified, dialyzed with injection buffer (10 mM Tris, pH 7.4, 0.2 mM EDTA) and filtered twice through a 0.22 µm filter (Millex-GV4, Millipore). They were diluted to 2–5 ng/µl in injection buffer and co-injected into pronuclei of fertilized F₂ (CBA × C57/B16) mouse eggs according to the protocol of Hogan et al. (Hogan et al., 1994). Transgenic animals were identified by Southern blot and PCR of genomic DNA from tail clippings. PCR were performed for 30 cycles of amplification at 94°C, for 1 minute, 52°C for 1 minute and 72°C for 1 minute. For Southern blot analysis, tail or yolk sacs DNA were digested with *BamHI* and electrophoresed on 1% agarose gel. Blots were hybridized as follows: prehybridization for 2 hours in 50% formamide, 6× SSPE, 5× Denhardt's solution, 25 mM phosphate pH 6.9, 0.3% SDS, 0.4 mg/ml of sonicated salmon sperm DNA and then hybridized with 10⁵ cpm probe/ml of prehybridization solution for 24 hours at 42°C. To identify transgenic animal, a 1 kb *BamHI* fragment was generated from the *Gcm1* cDNA and used as a probe. The presence of the *lacZ* transgene was then confirmed using a *lacZ*-specific probe.

X-gal staining and histology

Embryos between days 8.5 and 16.5 (days of vaginal plug was designated as day 0.5) were dissected in cold phosphate buffer (PBS) and fixed in 2% paraformaldehyde in 0.1 M Pipes (piperazine-N,N'-bis-2-ethanesulfonic acid; Sigma, St Louis, MO) pH 6.9 containing 2 mM MgCl₂ and 1.25 mM EGTA for 30 minutes at 4°C. Embryos were then washed in 0.1 M PBS containing 0.02% NP40 for 20 minutes and stained in the dark at 37°C in 1 mg/ml X-gal, 5 mM K₃Fe(CN)₆, 5 mM K₄Fe(CN)₆, 2 mM MgCl₂, 0.02% NP40 and 0.01% sodium deoxycholate in 0.1 M PBS pH 7.4. After the staining, embryos were washed in PBS and fixed in 4% paraformaldehyde overnight, cleared in 70% ethanol and photographed as whole mounts. They were then dehydrated and embedded in paraffin. Ten µm sections were cut, dewaxed and counterstained with 0.1% Eosin or with Hematoxylin and Eosin for histological examination of the embryos.

Northern blot

For northern blot analysis, total RNA were extracted from E9.5 transgenic and wild-type embryos using guanidine thiocyanate-cesium chloride method (Sambrook et al., 1989). Poly(A) selected RNA were purified on oligo(dT) resin using mRNA isolation kit (Ambion). RNA were then separated on 1% agarose gel in 6.3% formaldehyde containing buffers, transferred to nylon membrane (Nytran) and hybridized with a 810-bp *Gcm1*-specific cDNA probe-labeled by random priming (NEB blot). After hybridization with the *Gcm1* probe, the blot was stripped and probed with a *GAPDH*-specific probe used as standard control of RNA loading.

In situ hybridization

In situ hybridization was carried out on 10 µm paraffin sections of

embryos as described by Wilkinson (Wilkinson et al., 1987). The following probes were used to generate sense and antisense riboprobes: *Shh* probe corresponding to a 642-bp *EcoRI* fragment (a gift from Dr A. McMahon, Harvard University), *Pax3* probe [530-bp *PstI/HindIII* fragment from the 3'-end of the gene (Goulding et al., 1991)], *Gcm1* probe [800-bp fragment, bases 710–1510 in the sequence in Altshuller et al. (Altshuller et al., 1996)], *Tbx6* probe was generated from an EST clone (IMAGE consortium clone ID 1446422), *Fgfr1* probe, corresponding to a 400-bp fragment covering the Ig.II and 5' half of the Ig.III domains, was generated by PCR using *Fgfr1* cDNA as a template (a gift from Dr M. Goldfarb, Mount Sinai School of Medicine, New York), *Notch1* probe corresponds to a 422-bp fragment (a gift from Dr J. Kitajewski, Columbia University, New York, NY). Sense and anti-sense ³⁵S-UTP-labelled riboprobes were generated with T3 or T7 RNA polymerases using a standard in vitro transcription protocol.

Immunohistochemistry

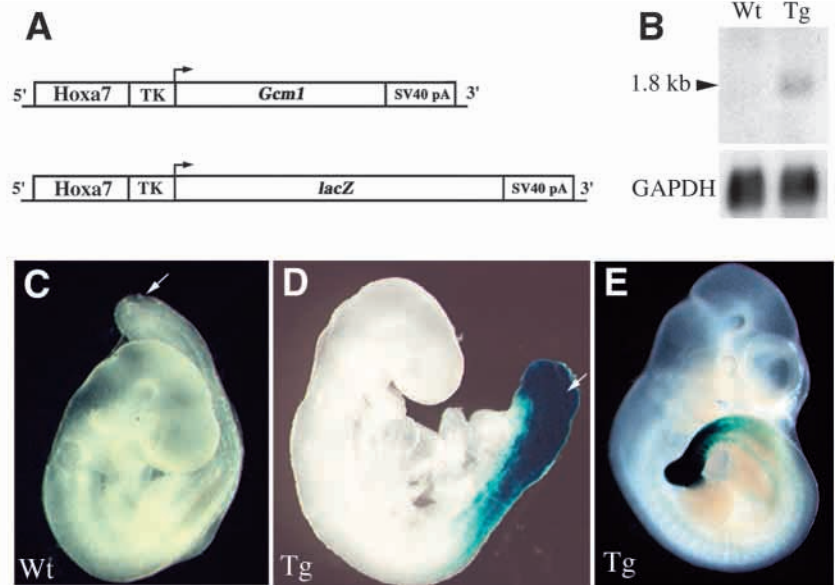
Embryos were dissected in cold PBS and fixed in 4% (w/v) paraformaldehyde overnight at 4°C and embedded in paraffin according to standard protocols. Ten µm sections were deparaffinized in xylene and hydrated through a graded ethanol series, then treated with 1% H₂O₂/10% methanol in 0.1 M PBS for 20 minutes, washed extensively in PBS and blocked for 1 hour in 10% normal goat serum, 1% gelatin, 5% BSA, 0.05% sodium azide in 0.1 M PBS. They were incubated overnight with the primary antibody diluted in 10% normal goat serum/0.1 M PBS in a humid chamber. Sections were then washed in 0.1 M PBS/0.1% Triton X-100 (Sigma) 3 time for 20 minutes and then incubated with the appropriate peroxidase-conjugated secondary antibody for 1 hour at room temperature. Sections were then washed in 0.1 M PBS/0.1% Triton X-100 and transferred in 0.1 M Tris-HCl pH 7.6. Peroxidase histochemistry was performed in 0.1 M Tris-HCl pH 7.6 containing 0.03% diaminobenzidine (DAKO, Carpinteria, CA), 0.1% NiCl₂ and 0.003% H₂O₂ and stopped in water. Sections were dehydrated, cleared in xylene and mounted in cytooseal (Stephens Scientific). The following primary antibody were used: a mouse monoclonal anti-Islet-1 (1/20 dilution, mouse IgG2b, 39.4D5; DSHB, University of Iowa), a mouse monoclonal anti-tubulin β3 (mouse IgG2b, clone SDL.3D10, 1/100 dilution; Sigma), a mouse monoclonal anti-MAP2 (mouse IgG1, 1/100 dilution; Sigma), and a mouse monoclonal anti-neurofilament 160 (mouse IgG1, 1/200 dilution; Sigma).

Magnetic resonance imaging

Each E16.5 embryo was positioned within a 1.5 cm diameter polyethylene tube filled with Fomblin (perfluoropolyether; Ausimont, Thorofare, New Jersey) used as a wetting and embedding agent to prevent dehydration and to reduce artifacts at tissue margins. Where present, air bubbles were aspirated from the interstices of the embryo with a very fine needle and syringe. The sample was wedged in place between two styrofoam plugs to reduce tissue vibration and the tube was sealed to prevent evaporation and re-entry of air bubbles.

The magnetic resonance images in the axial, coronal and sagittal planes were obtained on a 9.4 T superconducting magnet with a vertical 89 mm bore using a 25 mm birdcage coil. An automated water cooling system maintained the temperature within the bore at less than 30°C (Bruker Avance System with microimaging; Bruker Analytik, Rheinstetten, Germany). Pilot studies of diverse T₁, T₂ and intermediate-weighted (Int-w) sequences led us to select the Int-w sequence for spinal cord analysis, specifically: TR=2000 mseconds, TE=45 mseconds, slice thickness 0.5 mm, field of view 15×15 mm, data matrix 512×512, and number of excitations=50. This corresponds to an in-plane resolution of 29×29 µm and a slice thickness of 500 µm. Each sample was run overnight for a total acquisition time of 14 hours, 17 minutes.

Fig. 1. Expression pattern of the *Hoxa7-Gcm1* transgene. (A) A diagrammatic representation of the two transgenes used in this work (see Materials and Methods for details). A cDNA fragment containing the entire coding sequence of *Gcm1* (1.6 kb) is under the control of the 470-bp enhancer element of the mouse *Hoxa7* gene and thymidine kinase minimal promoter (TK). SV40 polyadenylation signal sequences terminate the transgene transcript. In a separate transgene, the *E. coli lacZ* gene replaces the *Gcm1* gene. (B) Northern blot of poly(A)-selected RNA from E9.5 wild-type and double transgenic embryos were probed for *Gcm1*. Expression of the *Gcm1* transgene was confirmed by the detection of 1.8 kb band corresponding to the predicted size of the transgene transcript. (C-E) Lateral views of a E9.5 wild-type embryo (C), a E9.5 transgenic embryo (D) and a E10.5 transgenic embryo (E) stained for β -galactosidase activity. The expression domain of the transgene is restricted to the caudal part of the embryo with an anterior boundary at the level of somite 18-20. At E9.5, note the enlargement of the posterior neuropore in the transgenic embryo as compared to the small oval shape of the posterior neuropore in wild type (arrow in C,D).



RESULTS

An experimental paradigm for transient, ectopic expression of *Gcm1*

In order to assess the effects of *Gcm1* during CNS development, we have generated transgenic mice expressing *Gcm1* and *lacZ* under the control of the mouse *Hoxa7* enhancer. The 470-bp *Hoxa7* enhancer was originally identified by Knittel et al. (Knittel et al., 1995) as a minimal control element specifying the anterior boundary of *Hoxa7* expression. This element directs expression in the developing tail bud during the period E9 to E13. The anterior boundary of *Hoxa7* expression starts at the hind limb bud and recedes rostrally with time, so that by E12.5 only the tip of the tail bud shows transgene expression. This element directs expression in most neuroepithelial and mesodermal derivatives in the caudal region. By limiting the transgene expression to the caudal region and to only a brief period, we hoped to diminish the likelihood of embryonic lethality due to transgene expression.

Five independent *Gcm1* founder transgenic mice were generated with these constructs (see Fig. 1A). In all animals, ectopic expression of *Gcm1* leads to congenital CNS abnormalities. Most analyses described here were carried out on two permanent transgenic lines that were established. To illustrate the domain of transgene expression, embryos (E9.5 to E16.5) bearing the *Hoxa7-lacZ* transgene were stained with X-gal as whole mounts. As shown in Fig. 1D,E, the expression of the *Hoxa7-Gcm1* transgene is detectable at E9.5 in the most caudal region of the embryos with an anterior limit of expression at the level of somite 18-20 (mid-thoracic level). β -galactosidase activity was observed in the neural tube and somites as well as in mesenchymal cells of the tail bud (Fig. 1D,E). A rostral-caudal gradient of *lacZ* activity is also noted at this stage. At E10.5, *lacZ* activity shifts caudally and remains robust in the tail bud (Fig. 1E). At later stages, β -galactosidase

staining is only detectable in the tail bud and in the tail until E12.5. Furthermore, expression of *Gcm1* in E9.5 transgenic embryos was confirmed by the detection on northern blots of a single transcript of 1.8 kb, which corresponds to the predicted size of the transgene mRNA (Fig. 1B).

Gcm1 expression induces severe neural tube malformations

Gross morphologic examination of transgenic embryos revealed two types of severe neural tube defects. All transgenic mice derived from the 5 founders showed either one or both of the two pathologic phenotypes: failure of neural tube closure (spina bifida) and the presence of ectopic neural tubes (diastematomyelia). A summary of the examination of 62 transgenic embryos, shown in Table 1, reveals that 100% of the embryos had multiple neural tubes and 26% had open neural tube. No signs of embryonic lethality were observed. Most remarkably the neonatal animals exhibit a progressive resolution of their spina bifida and by 2 months of age show no outward signs of the embryonic neural defect.

Neural tube closure defect

As early as E9.5, transgenic embryos showed an enlargement of the posterior neuropore as compared with the small oval

Table 1. Frequency of ectopic neural tubes and spina bifida in transgenic embryos

Stage	No. of transgenics	Spina bifida	Ectopic neural tubes
E9.5	7	3	7
E10.5	17	2	17
E12.5	20	7	20
E14.5	3	0	3
E16.5	15	4	15
Total	62	16 (25.8%)	62 (100%)

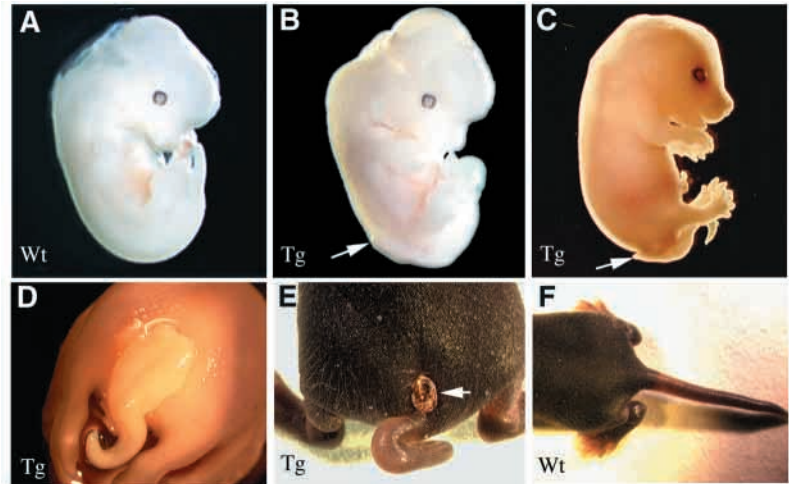


Fig. 2. The gross morphology of *Hoxa7-Gcm1* transgenic mice. (A,B) Lateral views of E12.5 wild-type (A) and transgenic (B) embryos. **The arrow in B indicates spina bifida in the transgenic embryo.** (C,D) Lateral and posterior aspect of a transgenic E16.5 embryo revealing a subcutaneous neural plate-like structure (arrow). (E,F) Posterior aspects of 1-week-old wild-type and transgenic littermates. Scarring and necrosis is evident in the transgenic pup (arrow).

shape of the posterior neuropore in wild-type embryos (Fig. 1C,D). This difference suggests an inhibition of the neural tube closure in the transgenic mice. Neural tube defects in the lumbo-sacral region were more obvious when E12.5-E16.5 embryos were examined (Fig. 2). The spina bifida extended from the level of the hind limb bud to the sacral region (Fig. 2B,C). The neural tube in this region remains flattened on the top of the ectoderm forming a neural placode, characteristic of the spina bifida aperta (Fig. 2D and Fig. 3A). At postnatal day 7, transgenic mice with this pathology showed a subcutaneous plate-like structure in the lumbo-sacral region with signs of necrosis (Fig. 2E). After the second postnatal week, this subcutaneous neural plate-like structure was totally resorbed and signs of scarring were no longer visible. Furthermore, all transgenic mice (100% penetrance) developed a kinky tail (Fig. 2E) unlike their wild-type littermates (Fig. 2F).

Multiple neural tubes

The second type of neural tube defects is revealed in histological examination of lumbo-sacral sections of transgenic embryos. Sections through this region showed the presence of ectopic neural tube structures (Fig. 3B), similar to human diastematomyelia. Two ectopic neural tubes were most frequently seen in the transgenic animals, but some had three or more. Serial sections revealed that the ectopic neural tubes were attached at their rostral end to the primary neural tube and formed a bifid spinal cord (data not shown). The presence of dorsal root ganglia associated with the primary neural tube at this level demonstrates that the ectopic tubes extended up to the region generated during primary neurulation. The ectopic neural tubes are confined to the region of the hind limb bud and tail bud. Frequently there is also a lipoma at the tip of the spinal cord (Fig. 3D,E), a characteristic also shared with the human spinal dysraphias. The physical relationship between the ectopic neural tubes and the neural tube closure defect can best be appreciated in the magnetic resonance images of an E16.5 transgenic embryo presented in Fig. 4. The ectopic neural tube can be seen emerging from the primary neural tube in the vicinity of the posterior neuropore where the neural tissue is hyperplastic and convoluted (Fig. 4D). The ectopic neural tube extends rostrally with progressively reduced

caliber to a level above the kidneys (Fig. 4A-C). The MR images also reveal evidence of a neural tube closure defect and the discontinuity of the surface ectoderm (arrowheads, Fig. 4C,D).

A second type of ectopic tubular structure is observed at the tip of the tail bud. Examination of serial histological sections through the tail bud of E12.5 transgenic embryos revealed the presence of ectopic tubular structures with a neuroepithelial-like feature (Fig. 5B) that were free floating and were not connected to the primary neural tube. The neuroepithelial identity of these ectopic tubular structures was confirmed by immunostaining for tubulin β 3 (Fig. 5C). The presence of ectopic neural tubes in this region suggests that ectopic expression of *Gcm1* in mesenchymal cells may promote the formation of secondary neural tubes by a process similar to secondary neurulation.

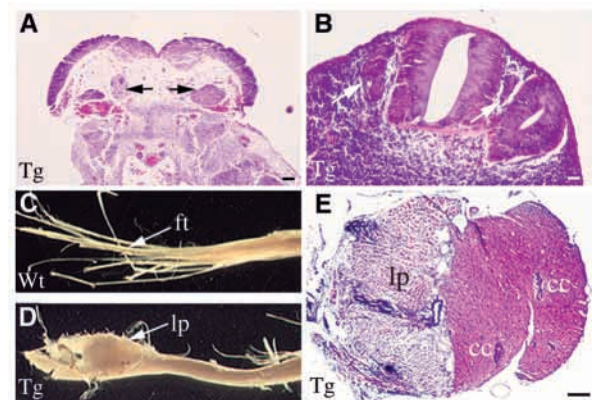
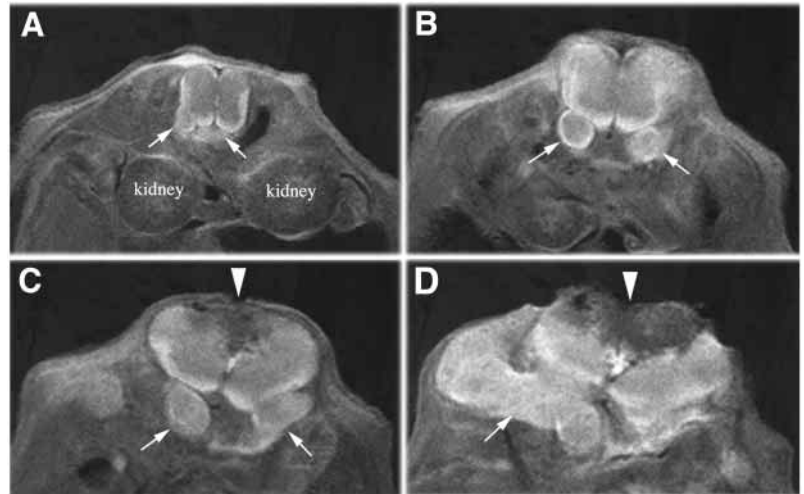


Fig. 3. Histologic analyses of the spina bifida and ectopic neural tubes in transgenic mice. (A,B) Transverse sections through the lumbo-sacral level of the spinal cord showing the histological features of the spina bifida (A) and an ectopic neural tube (B) in E12.5 transgenic embryos. Dorsal root ganglia are indicated by the arrows. (C,D) View of the filum terminale (ft) in 1-month-old wild-type (C) and transgenic (D) spinal cord. Note the presence of a lipoma (lp) in the transgenic spinal cord. (E) Transverse section of the adult transgenic spinal cord illustrating the attached lipoma and the split cord. cc, central canal; A,B,E, Hematoxylin and Eosin staining. Bars: 100 μ m.

Fig. 4. Magnetic resonance images of fixed, whole-mount transgenic embryos. The serial MRI transverse sections of an E16.5 transgenic embryo are arranged in a rostral (A) to caudal (D) series. The ectopic neural tubes (arrows) emerge ventrally from the spinal cord in the vicinity of the posterior neuropore (D) and proceed rostrally with progressively diminishing caliber to the level of the kidneys (A-C). The arrowheads in C and D indicate the area of spina bifida with a lesion in the surface ectoderm.



Patterning and cellular differentiation within the ectopic neural tubes

We assessed the neural identity, the cyto-architecture and the degree of differentiation within the ectopic neural tubes by *in situ* hybridization and immunomicroscopy. *In situ* hybridization was then performed to examine the dorsoventral properties of the endogenous and ectopic neural tubes of the transgenic embryos and compare it to that found in non-transgenic littermates. Sonic hedgehog, *Shh*, is a notochord and floor plate marker of the neural tube. *In situ* hybridization with *Shh* probes showed the presence of a single notochord in all wild-type embryos, and even transgenic embryos with three neural tubes, showed expression in all the neural tubes (Fig. 6A,C). Probes for the pair rule gene *Pax3* (a marker for dorsal neural tube and dermatomyotome) revealed expression in the expected domain of the primary neural tube of both the transgenic and non-transgenic embryos (Fig. 6B,D). However, expression of this marker in ectopic neural tubes was variable and appeared to depend upon the position of the tubes in the embryo. When the tubes lay close to the surface ectoderm of the embryo, they expressed *Pax3*. When they lay at a distance from the surface ectoderm, as in Fig. 6D, they did not express the marker, perhaps because the *Pax3* inducing BMP signal is not sufficiently strong at this remote location. Nonetheless, expression domains of *Shh* and *Pax3* appear normal in transgenic animals.

Immunomicroscopic analyses revealed that both the primary and ectopic neural tubes were differentiating and adopting the neural tube cyto-architecture apax with neural tubes in age-matched non-transgenic littermates. Tubulin $\beta 3$ - and MAP2-positive cells, which are presumptive differentiating neurons, formed the outer layer of the neural tube, while the cell layer adjacent to the central canal remained undifferentiated (Fig. 7A,B). In transverse sections of non-transgenic E12.5 embryos, *Islet-1* immunoreactivity is detected in the motoneuron precursors of the forming ventral horn of the spinal cord (Fig. 7C). In E12.5 transgenic embryo, *Islet-1* staining was detected in both its expected domain in the primary neural tube and also in two ventrally located ectopic neural tubes (Fig. 7D), indicating that motoneurons were developing in all of these structures.

Gcm1 restricts expression of mesodermal differentiation factors

We investigated the consequences of *Gcm1* expression in the tail bud of E9.5 wild-type and transgenic embryos by *in situ* hybridization. We were unable to detect any *Gcm1* mRNA in non-transgenic embryos (Fig. 8A). The absence of *Gcm1* mRNA in these tissues suggests that it does not play an important role in secondary neurulation. However, in the transgenic tail bud, transcripts of the *Gcm1* transgene were

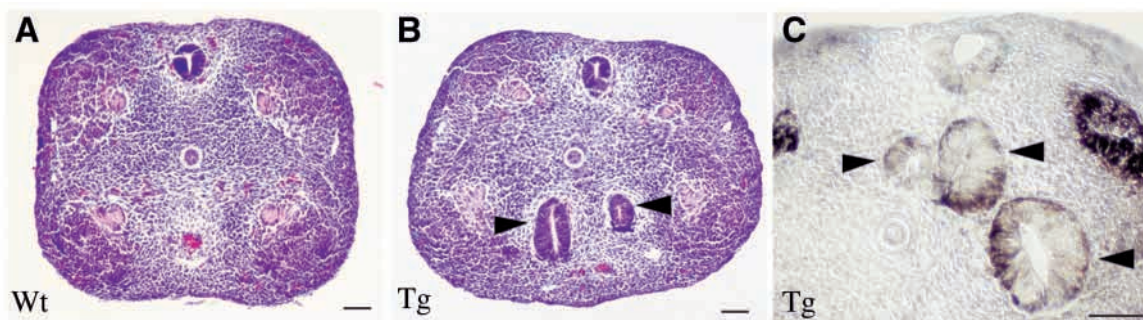


Fig. 5. Free-floating neural tubes in the transgenic tail buds. Transverse sections of E12.5 wild-type (A) and transgenic tail buds (B,C). In the transgenic tail bud, free-floating tubular structures (B, arrowheads) are formed in place of mesodermal tissues. Immunostaining for tubulin $\beta 3$ confirms the neural nature of the ectopic tubes in the transgenic tail bud (C). (A-C) Dorsal is at the top and ventral is at the bottom. (A,B) Hematoxylin and Eosin staining, (C) Immuno-peroxidase labeling. Bars: 100 μm .

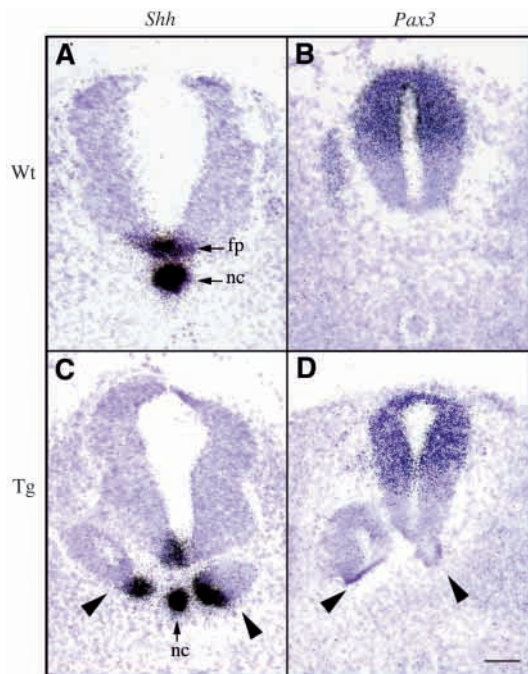


Fig. 6. Brightfield photomicrographs of *Shh* and *Pax3* expression in wild-type and transgenic neural tubes. ^{35}S -in situ hybridization for *Shh* (A,C) and *Pax3* (B,D) at E12.5. (A) *Shh* is expressed in the floor plate (fp) and notocord (nc) in the wild-type embryo. (C) In the transgenic embryos a single notocord is visible and each ectopic neural tubes (arrowheads) has a floor plate. (B,D) *Pax3* mRNA is normally expressed in the dorsal neural tube in wild-type (B) and transgenic (D) embryos. Ventrally located neural tubes (arrowheads) show no *Pax3* signal in the transgenic conceptuses. Bar: 50 μm .

easily detected in small clusters of cells condensing to form tubular structures inside the mesenchyme surrounding the hindgut (Fig. 8B). The *Gcm1* transgene is not expressed uniformly in the seemingly homogeneous mesenchyme but

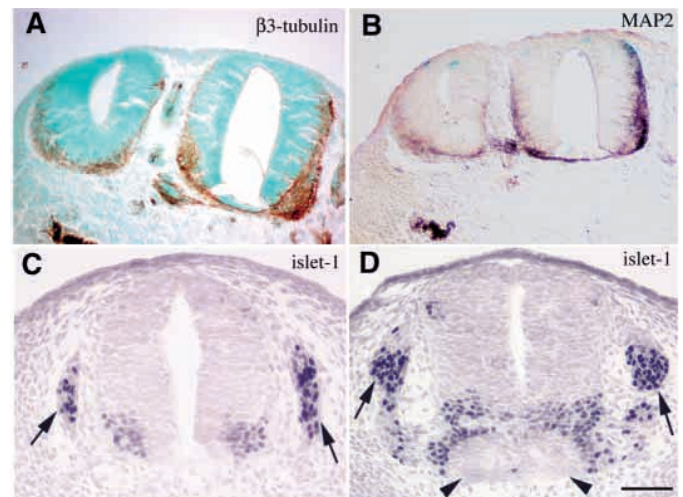


Fig. 7. Immunostaining reveals cellular differentiation within the ectopic neural tubes. Immunostaining for tubulin $\beta 3$ (A) and MAP2 (B) confirms the neural identity of the ectopic tubes in E12.5 transgenic embryos. (C,D) Differentiating motoneurons and dorsal root ganglia are identified by Islet-1 immunostaining in wild-type (C) and transgenic (D) neural tubes at E12.5. Ectopic neural tubes are indicated by arrowheads and dorsal root ganglia by arrows. Immunoperoxidase labeling was used in all sections. The section in A was counterstained with Methyl Green. Bar: 50 μm .

rather in discrete islands. Furthermore, the cells expressing *Gcm1* are driven toward a tubular organization. To further investigate this cellular diversity, we assessed the level and uniformity of *Fgfr1*, *Notch1* and *Tbx6* expression by in situ hybridization in both transgenic and non-transgenic E9.5 tail buds. These genes are essential for the specification of a mesodermal cell fate as previously reported (Beck and Slack, 1999; Chapman et al., 1996; Ciruna and Rossant, 2001). The expression of *Notch1* (Fig. 8E,F) and *Tbx6* (Fig. 8G,H) appears

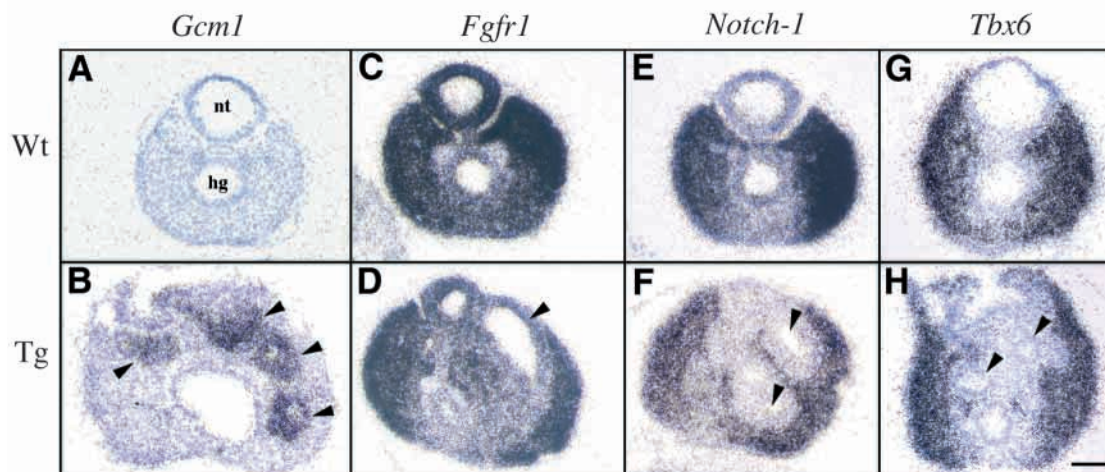


Fig. 8. *Gcm1* restricts expression of genes encoding mesodermal differentiation factors. Transverse sections through the tail bud of E9.5 wild-type (A,C,E,G) and transgenic (B,D,F,H) embryos were hybridized with *Gcm1* (A,B), *Fgfr1* (C,D), *Notch1* (E,F) and *Tbx6* (G,H) ^{35}S -labeled riboprobes, and then counterstained with Hematoxylin. In the transgenic tail bud, *Gcm1*-expressing cells form secondary neural tube-like structures (arrowheads, B). In contrast, no expression of *Gcm1* is detected in the wild-type tail bud (A). Expression levels of *Fgfr1*, *Notch1* and *Tbx6* are reduced in the secondary neural tubes of the transgenic tail buds (D,F,H). (H) The small rosettes of cells with no *Tbx6* expression are those that tend to form secondary neural tubes (arrowheads). Bar: 50 μm .

to be specifically excluded from the cells condensing into tubular structures.

The formation of the paraxial mesoderm depends on a transcriptional cascade that involves the FGFR1, Notch1 and *Tbx6* (Beck and Slack, 1999; Chapman et al., 1996; Ciruna and Rossant, 2001). The preferential exclusion of *Notch1* and *Tbx6* mRNAs from condensing mesenchymal cells and the expression of *Gcm1* in these same cells, suggests a reciprocal expression pattern in which ectopic expression of *Gcm1* overrides and suppresses a mesodermal cell fate, channeling the cells towards the default neural pathway.

DISCUSSION

The *glial cell missing* gene of *Drosophila* has been described as a master regulator of glial cell fate specification (Anderson, 1995). The mammalian homologues of *gcm* are expressed in both neural and non-neural tissues and they appear to participate in the specification of several diverse cell fates. In the present study, we show that transient expression of *Gcm1* in the developing tail bud consistently leads to two severe neural tube defects: a neural tube closure defect (spina bifida) and the induction of ectopic neural tubes (diastematomyelia).

The transgene that we employed initiates expression of *Gcm1* at a time and place that are of critical importance to neurulation: E9.5 and the tail bud, the time and place of the posterior neuropore closure and secondary neurulation (Nievalstein et al., 1993; Schoenwolf, 1984). At that time the caudal tip of the neural tube lies adjacent to the tail bud (Griffith et al., 1992). The embryonic tail bud comprises a seemingly homogeneous mass of cells and represents the remains of Hensen's node and the primitive streak. This cell mass has remarkable developmental potential and gives rise, during subsequent development, to a variety of structures including the secondary neural tube, the caudal notochord, hind gut, part of the vertebral column and musculature; all without the previous formation of the three germ layers (Griffith et al., 1992; Tam and Trainor, 1994). This seemingly direct generation of ecto-, endo- and mesodermal cell types is in stark contrast to the generation of similar cell types in the rostral regions, and the details of this process are incompletely understood.

After closure of the posterior neuropore (E9.5-10) the primary neural tube is extended caudally through a process of secondary neurulation (Naidich et al., 1996; Nievelstein et al., 1993; Schoenwolf, 1984). At that time the closed primary neural tubes extends to the level of somite 32-34, the future level of the third sacral vertebra and thus primary neurulation forms the parts of the wild-type spinal cord that have dorsal and ventral roots. The secondary neurulation produces the caudal spinal cord, including the portions that are the primordia of the filum terminale, the ventriculus terminalis and part of the conus medullaris. In mice, the observed earliest event in secondary neurulation is the continuous accretion of aggregates of the tail bud mesenchymal cells in the form of medullary rosettes at the caudal end of the primary neural tube (Muller and O'Rahilly, 1987; Muller and O'Rahilly, 1988; Nievelstein et al., 1993; Schoenwolf, 1984). These cells take on a columnar epithelial appearance and form a neurocoele by cavitation, the lumen being always in contact with the lumen of the primary neural tube.

Several lines of evidence suggest that the complex phenotype of the transgenic mice described here (spina bifida and diastematomyelia) is a direct result of two distinct phenomena: the inhibition of posterior neuropore closure and the indirect stimulation of secondary neurulation. That the spina bifida observed in the transgenic mice results from an inhibition of neuropore closure by *Gcm1* is supported by our estimates of the anatomical level of the defect. The position of the closure defect in affected transgenic mice, whether visualized in histologic sections or in whole mounts by MR imaging, is same in different animals and corresponds to the position of the posterior neuropore. The value of 26% reported in Table 1 for the proportion of transgenic embryos with recognizable spina bifida may be strongly affected by two competing secondary processes: progressive resolution of the defect and the neuroepithelial hyperplasia, which exaggerates the defect.

The possibility that *Gcm1* directly stimulates secondary neurulation is difficult to reconcile with our inability to detect any *Gcm1* mRNA in the wild-type tail bud during active secondary neurulation (Fig. 8). Rather, we believe that the transgene-derived *Gcm1* indirectly stimulates secondary neurulation that results in the generation of ectopic neural tubes. This hypothesis is supported by two lines of evidence. The time and place of transgene expression indicate that the ectopic neural tubes are not derived from primary neurulated tissue. Further, the appearance of numerous, small "free-floating" neural tube-like structures at the very tip of the tail bud suggests that the transgene-derived *Gcm1* stimulates the neuroepithelial differentiation of tail bud mesenchyme, a process already underway at that time and place. There is mounting evidence to suggest that when tail bud mesenchymal cells are prevented from differentiating into paraxial mesoderm they follow a pathway leading to the formation of secondary neural tubes. Much of the evidence comes from studies of the effects of mutations in the transcriptional or signaling factors known to be active in the mesenchyme to paraxial mesoderm transformation, an early stage in the differentiation of somites. Transcriptional cascades initiated by FGFR1 (Ciruna and Rossant, 2001) or *Wnt3a* (Yamaguchi et al., 1999a; Yamaguchi et al., 1999b; Yoshikawa et al., 1997) have been identified in the somite progenitor cells. Interruption of these cascades by null mutations in the genes encoding them leads not only to a deficit in paraxial mesoderm but also to the formation of ectopic neural tubes. Thus mutations in either *Fgfr1* (Ciruna et al., 1997; Deng et al., 1997), *Wnt3a* (Yoshikawa et al., 1997), *Tbx6* (Chapman and Papaioannou, 1998) or mutations in both *Lef1* and *Tcf1* (Galceran et al., 1999) lead to the formation of ectopic neural tubes. The transformation of paraxial mesoderm progenitors to neural progenitors that is apparent in these null mutants has been attributed to diversion of the progenitor cells to a default neural pathway when mesodermal differentiation is inhibited. Our results are compatible with this interpretation if ectopic expression of *Gcm1* in tail bud mesenchymal cells specifically interferes with their differentiation to paraxial mesoderm. *Gcm*-induced interference with both epidermal and mesodermal differentiation has been observed in *Drosophila* (Akiyama-Oda et al., 1998; Bernardoni et al., 1998; Reifegerste et al., 1999). In our study, we showed that ectopic expression of *Gcm1* in multipotential mesenchymal cells induces the down regulation of two factors normally required

for mesodermal differentiation, Notch1 and Tbx6, in cells assuming neuroepithelial cell type. We believe that the ectopic neural tubes in our transgenic mice result from the incomplete suppression of the differentiation of mesenchyme to paraxial mesoderm and the diversion of precursors to the default neural pathway. However the possibility that Gcm1 may directly induce neural-specifying genes can not be ruled out.

A striking difference between our transgenic mice and those bearing the aforementioned null mutations is that our transgenic animals are viable, fertile and live a normal life span. They show no obvious signs of posterior limb weakness. All mesoderm-derived organs and tissues are present in normal amount. Thus, the cells fated to the ectopic neural tubes seem to be in addition to, not instead of, paraxial mesoderm tissues. Thus, we further speculate that this interference with mesenchymal cell differentiation occasions a limited hyperplasia that brings the paraxial mesoderm generation to the normal range and accounts for the increase in neuroepithelial cells that we see in the transgenic embryos. These results are corroborated by the observation that the tail buds of E9.5 transgenic mice are consistently larger than those of their wild-type littermates. This hyperplasia seems restricted to the neuroepithelium and is evident in the MRI images of Fig. 4.

We are grateful to Dr K. Kelley for invaluable assistance in the generation of the transgenic mice and to Drs V. Friedrich and S. Henderson for advice with the microscopy imaging. We thank Dr R. DeGasperi and L. Burdine for excellent technical help. This work was supported by grants from NIH RO1 NS39836 (R. A. L.) and the National MS Society FA1363-A-1 (B. N. O.).

REFERENCES

- Akiyama, Y., Hosoya, T., Poole, A. M. and Hotta, Y. (1996). The gem-motif: a novel DNA-binding motif conserved in *Drosophila* and mammals. *Proc. Natl. Acad. Sci. USA* **93**, 14912-14916.
- Akiyama-Oda, Y., Hosoya, T. and Hotta, Y. (1998). Alteration of cell fate by ectopic expression of *Drosophila* glial cells missing in non-neural cells. *Dev. Genes Evol.* **208**, 578-585.
- Altshuler, Y., Copeland, N. G., Gilbert, D. J., Jenkins, N. A. and Frohman, M. A. (1996). Gcm1, a mammalian homolog of *Drosophila* glial cells missing. *FEBS Lett.* **393**, 201-204.
- Anderson, D. J. (1995). A molecular switch for the neuron-glia developmental decision. *Neuron* **15**, 1219-1222.
- Anson-Cartwright, L., Dawson, K., Holmyard, D., Fisher, S. J., Lazzarini, R. A. and Cross, J. C. (2000). The glial cells missing-1 protein is essential for branching morphogenesis in the chorioallantoic placenta. *Nat. Genet.* **25**, 311-314.
- Basyuk, E., Cross, J. C., Corbin, J., Nakayama, H., Hunter, P., Nait-Oumesmar, B. and Lazzarini, R. A. (1999). The murine *Gcm 1* gene is expressed in a subset of placental trophoblast cells. *Dev. Dyn.* **214**, 303-311.
- Beck, C. W. and Slack, J. M. (1999). A developmental pathway controlling outgrowth of the *Xenopus* tail bud. *Development* **126**, 1611-1620.
- Bernardoni, R., Miller, A. A. and Giangrande, A. (1998). Glial differentiation does not require a neural ground state. *Development* **125**, 3189-3200.
- Chapman, D. L., Agulnik, I., Hancock, S., Silver, L. M. and Papaioannou, V. E. (1996). Tbx6, a mouse T-Box gene implicated in paraxial mesoderm formation at gastrulation. *Dev. Biol.* **180**, 534-542.
- Chapman, D. L. and Papaioannou, V. E. (1998). Three neural tubes in mouse embryos with mutations in the T-box gene Tbx6. *Nature* **391**, 695-697.
- Ciruna, B. and Rossant, J. (2001). FGF signaling regulates mesoderm cell fate specification and morphogenetic movement at the primitive streak. *Dev. Cell.* **1**, 37-49.
- Ciruna, B. G., Schwartz, L., Harpal, K., Yamaguchi, T. P. and Rossant, J. (1997). Chimeric analysis of fibroblast growth factor receptor-1 (Fgfr1) function: a role for FGFR1 in morphogenetic movement through the primitive streak. *Development* **124**, 2829-2841.
- Deng, C., Bedford, M., Li, C., Xu, X., Yang, X., Dunmore, J. and Leder, P. (1997). Fibroblast growth factor receptor-1 (FGFR-1) is essential for normal neural tube and limb development. *Dev. Biol.* **185**, 42-54.
- Galceran, J., Farinas, I., Depew, M. J., Clevers, H. and Grosschedl, R. (1999). Wnt3a^{-/-} like phenotype and limb deficiency in Lef1(-/-)Tcf1(-/-) mice. *Genes Dev.* **13**, 709-717.
- Goulding, M. D., Chalepakis, G., Deutsch, U., Erselius, J. R. and Gruss, P. (1991). Pax-3, a novel murine DNA binding protein expressed during early neurogenesis. *EMBO J.* **10**, 1135-1147.
- Griffith, C. M., Wiley, M. J. and Esmond, J. S. (1992). The vertebrate tail bud: three germ layers from one tissue. *Anat. Embryol.* **185**, 101-113.
- Hogan, B., Beddington, R., Costantini, F. and Lacey, E. (1994). *Manipulating the Mouse Embryo*. New York: Cold Spring Harbor Laboratory Press.
- Hosoya, T., Takizawa, K., Nitta, K. and Hotta, Y. (1995). glial cells missing: a binary switch between neuronal and glial determination in *Drosophila*. *Cell* **82**, 1025-1036.
- Jones, B. W., Fetter, R. D., Tear, G. and Goodman, C. S. (1995). glial cells missing: a genetic switch that controls glial versus neuronal fate. *Cell* **82**, 1013-1023.
- Kim, J., Jones, B., Zock, C., Chen, Z., Wang, H., Goodman, C. and Anderson, D. (1998). Isolation and characterization of mammalian homologs of the *Drosophila* gene *glial cells missing*. *Proc. Natl. Acad. Sci. USA* **95**, 12364-12369.
- Knittel, T., Kessel, M., Kim, M. H. and Gruss, P. (1995). A conserved enhancer of the human and murine Hoxa-7 gene specifies the anterior boundary of expression during embryonal development. *Development* **121**, 1077-1088.
- Muller, F. and O'Rahilly, R. (1987). The development of the human brain, the closure of the caudal neuropore, and the beginning of secondary neurulation at stage 12. *Anat. Embryol.* **176**, 413-430.
- Muller, F. and O'Rahilly, R. (1988). The development of the human brain from a closed neural tube at stage 13. *Anat. Embryol.* **177**, 203-224.
- Naidich, P. T., Zimmerman, A. R., McLone, G. D., Raybaud, A. C., Altman, R. N. and Braffman, H. B. (1996). Congenital anomalies of the spine and spinal cord. In *Magnetic Resonance Imaging of the Brain and Spine* (ed. W. S. Atlas). Philadelphia: Lippincott-Raven.
- Nievelstein, R. A. J., Hartwig, N. G., Vermeij-Keers, C. and Valk, J. (1993). Embryonic development of the mammalian caudal neural tube. *Teratology* **48**, 21-31.
- Reifegerste, R., Schreiber, J., Gulland, S., Ludemann, A. and Wegner, M. (1999). mGCMa is a murine transcription factor that overrides cell fate decisions in *Drosophila*. *Mech. Dev.* **82**, 141-150.
- Sambrook, J., Fritsch, E. and Maniatis, T. (1989). *Molecular Cloning*, 2nd ed. Cold Spring Harbor, New York: Cold Spring Harbor Laboratory Press.
- Schoenwolf, G. C. (1984). Histological and ultrastructural studies of secondary neurulation in mouse embryos. *Am. J. Anat.* **169**, 361-376.
- Schreiber, J., Sock, E. and Wegner, M. (1997). The regulator of early gliogenesis glial cells missing is a transcription factor with a novel type of DNA-binding domain. *Proc. Natl. Acad. Sci. USA* **94**, 4739-4744.
- Schreiber, J., Enderich, J. and Wegner, M. (1998) Structural requirements for DNA binding of GCM proteins. *Nucleic Acids Res.* **10**, 2337-2343.
- Schreiber, J., Riethmacher-Sonnenberg, E., Riethmacher, D., Tuerk, E. E., Enderich, J., Bosl, M. R. and Wegner, M. (2000). Placental failure in mice lacking the mammalian homolog of glial cells missing, GCMa. *Mol. Cell. Biol.* **20**, 2466-2474.
- Tam, P. P. and Trainor, P. A. (1994). Specification and segmentation of the paraxial mesoderm. *Anat. Embryol.* **189**, 275-305.
- Wilkinson, D. G., Bailes, J. A., Champion, J. E. and McMahon, A. P. (1987). A molecular analysis of mouse development from 8 to 10 days post coitum detects changes only in embryonic globin expression. *Development* **99**, 493-500.
- Yamaguchi, T. P., Bradley, A., McMahon, A. P. and Jones, S. (1999a). A Wnt5a pathway underlies outgrowth of multiple structures in the vertebrate embryo. *Development* **126**, 1211-1223.
- Yamaguchi, T. P., Takada, S., Yoshikawa, Y., Wu, N. and McMahon, A. P. (1999b). T (Brachyury) is a direct target of Wnt3a during paraxial mesoderm specification. *Genes Dev.* **13**, 3185-3190.
- Yoshikawa, Y., Fujimori, T., McMahon, A. P. and Takada, S. (1997). Evidence that absence of Wnt-3a signaling promotes neuralization instead of paraxial mesoderm development in the mouse. *Dev. Biol.* **183**, 234-242.